



	<b>Experiment title:</b> <b>Metal Structures in 4D</b>	<b>Experiment number:</b> ME-1162
<b>Beamline:</b> ID11	<b>Date of experiment:</b> from: 1/9 2005 to: 1/1 2008	<b>Date of report:</b> 15/1/2007  <i>Received at ESRF:</i>
<b>Shifts:</b>	<b>Local contact(s):</b> L. Margulies, J. Wright, G. Vaughan, C. Gundlach	
<b>Names and affiliations of applicants (* indicates experimentalists):</b> H.F. Poulsen*, L. Margulies*, S. Schmidt*, E.M. Lauridsen*, S.F. Nielsen*, D. Juul Jensen, G. Winther, W. Pantleon  Center for Fundamental Research: Metal Structures in 4D, Risoe National Laboratory, Technical University of Denmark., Dk-4000 Roskilde.		

This report highlights the research from the first 2 years of work within LTP ME-1162. This LTP is the continuation of a long standing collaboration between the group at Risø and ID11 on the development and proliferation of the technique now known as Three-Dimensional X-Ray Diffraction (3DXRD). Starting in 1997 pioneering optics for hard x-rays were developed and first feasibility experiments demonstrated. This lead to the commisioning of the 3DXRD microscope at ESRF in 2000, an instrument funded by and built at Risø. During the years the technique rapidly developed, the user group expanded and with time the ID11 staff took over more of the external user guidance. Following the last beamline review of ID11 it was decided to completely refurbish the beamline and install two 3DXRD instruments in a new hutch; the existing one for work on larger samples and a spatial resolution of 1  $\mu\text{m}$  or above and a new nanoscope for small samples and resolutions down to 100 nm. This upgrade is seen as a pilot study for the ESRF upgrade and the 3DXRD work.

When formulating the current LTP, it was therefore intimately tied to the plans for the beamline upgrade, and in particular the establishment of the 3DXRD nanoscope. With respect to the instrumental work, Risø is mainly to be responsible for detectors and software algorithms, while ESRF staff are in charge of the general upgrade plans including optics and the nanoscope. Implementation of software and user guidance was seen as a shared effort.

Substantial delays have occurred in terms of optics and nano-manipulation. An improved set of focussing optics (KB mirror and refrative lense) were to be installed in the second hutch during the winter shutdown 2005. In the end, these optics installed in the newly extended hutch during the winter shutdown 2007 and

became available for experimental use in spring 2007. In addition, a new double bent Laue monochromator was to be installed during the summer shutdown of 2006. It has just recently been installed during the 2007 winter shutdown, and is currently in the final stages of commissioning. As these optical components were foreseen as critical for the development of the nanoscope, the construction and commissioning of this instrument has been pushed to 2009. During transition from the second hutch to the newly built extension there was a period of approximately 6 months when the beamline was no longer operating in user mode for 3DXRD experiments (the first hutch was still available, but is not suited to any of the experiments in our proposal).

Due to these unforeseen delays, which were outside our control, we have had to revise the experimental plan. Some basic metal science studies with the 3DXRD microscope had to be shifted until the instrument was commissioned again in the new hutch and the relevant optics was available. As the double bent Laue monochromator is a key element, in practice a number of key studies will be performed Spring and Summer 2008. Likewise all scientific studies with the nanoscope are shifted to the next LTP period. Instead more beamtime than expected has been used for tests and demonstrations in connection with the instrumental developments. This work has been accelerated by the EU 6<sup>th</sup> framework programme TotalCryst, which started February 2006, with H.F. Poulsen as PI and ESRF as partner. This programme specifically aims at generalising the 3DXRD concept for use in other fields such as chemistry, pharmacy and structural biology and at facilitating generation of user friendly software. In practice TotalCryst has provided 6 post docs mainly for instrumental work, two of which are placed at ID11. Below we present the status for the Risø lead activities on detector and software developments and provide a selection of research highlights during this period.

### **High spatial resolution detectors**

The main limitation to 3DXRD performance is the nearfield high spatial resolution detector. Due to lack of commercial players, the group has had to develop its own detectors since the beginning of the 3DXRD work. In the previous LTP period (2003-2005) the highest spatial resolution detector available had a pixel size of 4.3 microns, and a point spread function of approximately 16 microns. Within ME-1162, a new detector was built at Risø and successfully commissioned at ID11. This is based on the same type of technology, but with a pixel size of 1.3 microns and a point spread function of approximately 5 microns. It is clear, though, that to achieve even higher resolution a fundamentally new design has to be developed. One such design has shown great promise and is described below.

### **Structured Scintillators**

Currently, 2D detectors comprising a homogeneous fluorescence screen coupled by optics to a CCD system are used almost universally at synchrotrons for imaging purposes. However, to obtain a resolution in the 1 micron region, very thin phosphor screens are needed. As a result the efficiency of such detectors are poor (<3% at 50keV), which deteriorate the time-resolution of in situ experiments.

As an alternative design we propose to replace the homogeneous screen with a waveguiding structure, which collimates the visual light. This leads to three distinct advantages:

- The thickness of the screen may be 1-2 orders of magnitude larger for a given resolution
- A single depth of focus enables the use of high NA lenses, which contributes even further to improving the efficiency.
- MC simulations demonstrate that the tails are suppressed by orders of magnitude

More specifically, in collaboration with KTH in Stockholm, we have pursued R&D in structured scintillators based on electrochemical etching in silicon. Large (cm-sized) areas have been made with regular arrays of very deep and narrow pores (see Fig 1). A layer of SiO<sub>2</sub> is grown on the pore walls and CsI:Tl is melted into the pores, resulting in a structure with a high refractive index core surrounded by a quartz cladding, providing efficient light guiding. In this way the thickness of the structured scintillator does not degrade the resolution as it would with a conventional scintillator screen. A structure with 120 μm thickness and 4 μm pitch was tested at ESRF, and it was demonstrated that the spatial resolution and efficiency match simulations within error bars. In comparison to the existing detectors the efficiency is enhanced by more than a factor of 10. The

homogeneity was better than 7% while radiation damage was found to be negligible for doses up to at least  $2 \times 10^4$  Gy. More recently, structures with a pitch of  $1.4 \mu\text{m}$  have been developed, but have yet to be tested. This work is partly financed also by ID15, who aims at using the scintillators for fast tomography.

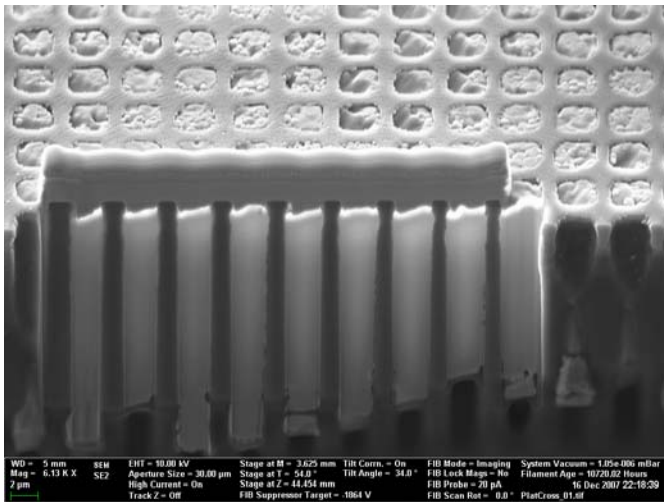


Fig. 1. Cross-section by FIB of top part of wave-guiding scintillator with pore distance of  $4 \mu\text{m}$ ,

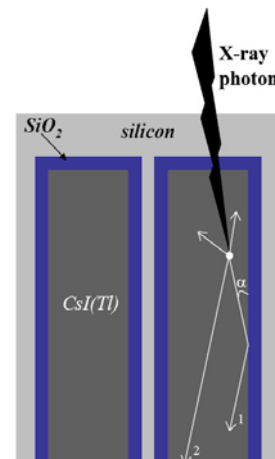


Fig. 2. Schematic of waveguiding scintillator. The silicon is largely transparent to hard X-rays, while the  $\text{SiO}_2$  confines the emitted visible light

Plans for 2008 include the construction of a 3D high resolution camera design which will utilize 2 screens in series, and being semi-transparent to allow for detection of diffracted rays at 2 high resolution screens in the near field and one large area detector (Frelon) in the far field. This will not only greatly increase the speed of data acquisition as all images will be collected simultaneously, but allow for greater stability since no detectors will have to be moved during an experiment. Furthermore, two detectors allow the application of so-called super resolution algorithms, well-known from image analysis. Such algorithms were tested at ID11 in 2007.

## Algorithms

The collaborative plan for software development is detailed in the EU grant proposal. The proposal itself as well as the half-term report – which was due August 2007 – can be found at [www.totalcryst.dk](http://www.totalcryst.dk). The work is progressing according to plan, with the validity of a number of new ideas being demonstrated, typically first by full-scale simulations and then by tests at ID11.

## Indexing

The program GRAINDEX – developed by Risø in 2001 – has been the workhorse for 3DXRD experiments. It enables indexing of several hundred grains within a polycrystal, but has several drawbacks, e.g. the run time may be half an hour, which prohibits on-line analysis. To overcome these drawbacks a new indexing program, GrainSpotter, has been developed. GrainSpotter is a pattern-recognition program that compares a list of measurements (G-vectors in reciprocal space) with a list of theoretical G-vectors. The discrete set of rotations that brings the set of theoretical scattering vectors onto a subset of the measured g-vectors are the crystallographic orientations of the grains present in the material.

Based on simulations in favourable conditions  $> 700$  grains can be recovered simultaneously without error. The run-time is in the second range. Grainspotter has been used for indexing of numerous experimental data sets from ID11 already, including – for the first time – the indexing of polycrystals with large unit cells, such as small proteins. Very recently, the Grainspotter algorithm has also been extended to allow indexing of samples with unknown space groups, a main concern for use in e.g. pharmacy (publications in preparation).

## 3D reconstruction of grain maps and orientation maps

Several new – and mathematically quite different – approaches have been pursued for 3D reconstruction of orientation maps (the 3D equivalent to the 2D OIM maps made with an electron microscope).

The new workhorse is *GrainSweeper* - a standalone program for reconstructing grain maps. The current resolution, which is limited by detector resolution, is 5 microns. Once the geometric (also called the global) parameters of the experimental setup are determined (beam energy, distance and tilt of the detector) the GrainSweeper program runs fully automatically. Data are collected using a planer beam shape thus illuminating a layer with thickness of typically 2-5 microns. Following the reconstruction a 2D voxel grid with crystallographic orientations is obtained (i.e. the output data format is similar to a grain map obtained by the electron back scattering method). By translating the sample vertically a full 3D data set is collected. The SweepMerge program merges the layers into a 3D volume. At the ID11 beamline the GrainSweeper runs on a computer cluster where all the layers are reconstructed in parallel. An example of an application is given below.

The output from GrainSweeper can be passed to other programs, which can be shown to provide superior reconstructions, but cannot stand alone. In collaboration with the applied mathematical groups at City University of New York (CUNY) and University of Leiden, our group has introduced *discrete tomography* as a new tool. Several programs have been completed and put to test at ID11. As an example we present results of simulations on an algorithm due to J. Batenburg. Simulations demonstrate that *perfect* reconstructions are possible, even in the presence of substantial noise, and even when as few as five diffraction spots per grain are available. Furthermore the run time is less than one second per layer on a standard PC. This should be compared with typical runtimes of hours for traditional approaches e.g. in tomography (publication in preparation).

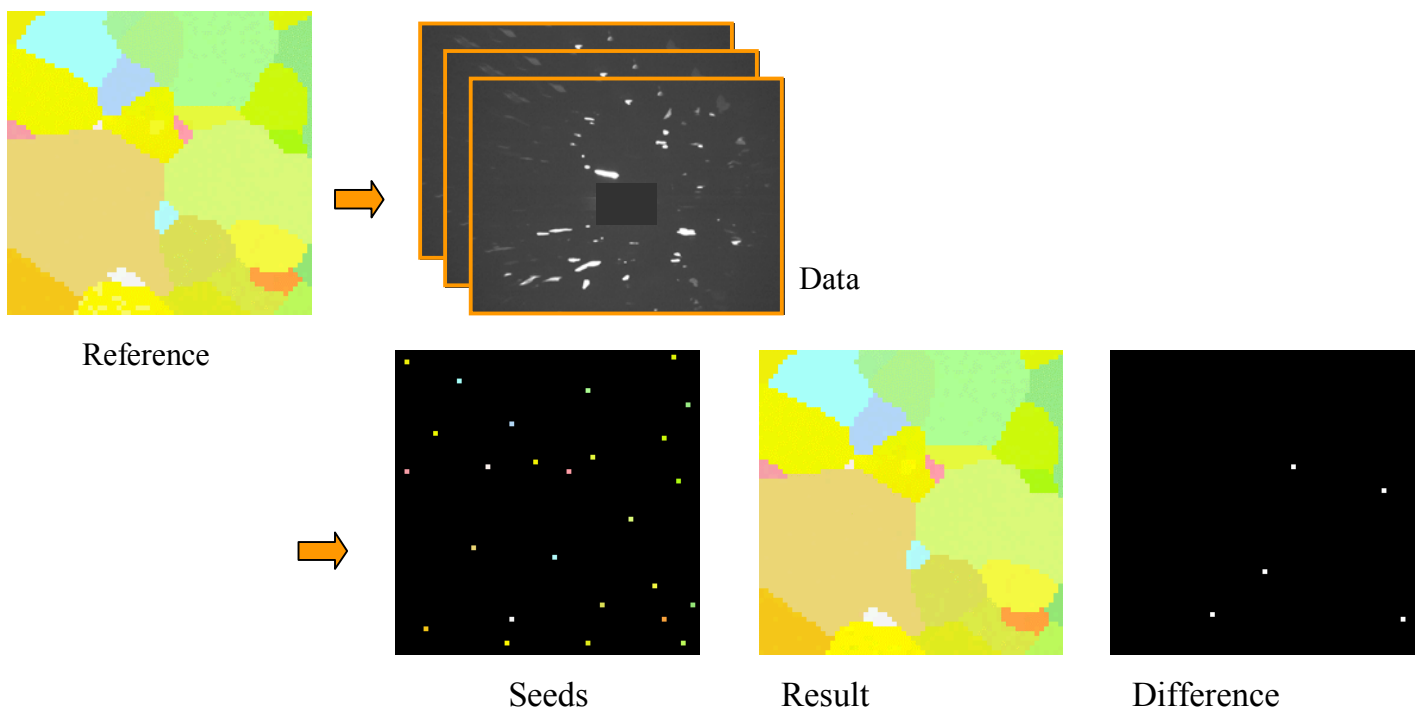


Figure 3. Validation of a reconstruction algorithm for 3D orientation maps of moderately deformed polycrystals. The colours in the reference symbolises orientations (note the gradient within grains). Based on this diffraction patterns are simulated. Given seeds within each grain, the MC reconstruction method “grows the grains”. The difference map shows the voxels not having the correct orientation.

The above reconstruction programs only applies to undeformed or slightly deformed microstructures, where all voxels within a given grain have (almost) the same orientation. To enable reconstruction of orientation maps also for moderatley deformed specimens, a Monte Carlo based approach has been developed with CUNY. The performance is demonstrated by simulations as shown in Figure 3. Experimentally a range of data sets have been acquired of Al and Cu polycrystals cold rolled to between 4% and 40%. The data analysis is still in progress.

Experimentally, the main problem for 3D reconstruction in general turned out to be the determination of the absolute geometry of the set-up (detector tilts etc) with sufficient precision. Recently, J. Wright from the beamline solved this problem elegantly in terms of a standardised calibration procedure.

### **Overcoming spot overlap**

One limitation to the above mentioned indexing algorithm is spot overlap. When there are many grains in the illuminated volume, spots will start to overlap, which eventually will imply that that spots cannot be indexed nor harvested for intensities. To overcome this problem, we suggest to first derive an orientation distribution function for each grain, then project this distribution onto the detector plane and use this projection for peak fitting. In this way spots superposed of signals from several grains can be separated. This is seen as crucial for solution and refinement applications in chemistry and pharmacy (see below) as the spot density increases with  $Q$ . The relevant program has just been completed (publication submitted), and is presently being applied to various experimental data sets on small, medium and large unit cells materials.

### **Box scan**

One of the main limitations to the above “3D reconstruction of grain map” algorithms is that the distance between sample and detector can only be a few millimeters. This complicates bulky sample environments like high temperature furnaces. To overcome these restrictions we present here an outline of an alternative measuring procedure, termed the beam scanning technique. This is suitable for non-destructive determination of 3D center-of-mass (CMS) coordinates, volume, crystallographic orientation and phase, but at this stage without detailed information about grain morphology. This new technique relies on use only of the farfield detector, that is the standard 2D CCD, allows therefore for bulky sample environments. Furthermore one can reach sub-micron spatial resolution, only limited by the step size of the sample translations. This becomes particularly interesting with the recent upgrade of ID11 towards a stable nano-focused beam.

The concept of the beam scanning technique is sketched in Figure 4. First, a series of scans is performed in the direction perpendicular to the beam ( $y$  in the lab frame at  $\omega=0$ ) using a vertical beam profile where for each point in the scan, a series of images are acquired corresponding to a range of sample positions translated in the parallel beam direction ( $x$  in the lab frame at  $\omega=0$ ), preferably spanning  $90^\circ$ . Next an identical set of scans is performed in the  $z$ -direction using a horizontal planar beam profile. By monitoring the integrated intensity of an associated diffraction spot as a function of position, the projected CMS position of the grain in the direction of the scan is found (cf. Fig. 4(a)). The ( $x, y, z$ ) CMS position can now be found by combining the  $y$ - and  $z$ -scans for two or more diffraction spots arising from the same grain. It is notable that the accuracy of the CMS position determined this way can be substantially better than the spatial resolution of the setup. Furthermore, the acquired projections can be used to extract some information on the shape of the grains, such as, for example, the moment of inertia or the aspect ratio. The sorting of the acquired projections according to their grain of origin can e.g. be accomplished using the multi-grain indexing software Grainspotter (cf. Fig. 4(c)). As an end result of this technique, all grains within the scanned volume are characterized with respect to their CMS position, moments of inertia, volume, crystal orientation and (optionally) strain (cf. Fig. 4(d)). It should be emphasized that the number of data acquisitions required for this technique is  $2NM$ , where  $N$  is the average number of steps in the  $y$ - and  $z$ -scans and  $M$  is the number of  $x$ -settings. In contrast, a true point-to-point 3D scanning procedure with a monochromatic beam would require  $N^3M$  acquisitions. Two experimental data sets have been acquired to validate the technique. These involve up to 10,000 grains. Currently a sub-set with some thousand grains has been indexed and positions found by a manual procedure. Further analysis is awaiting the completion of an automatic routine.

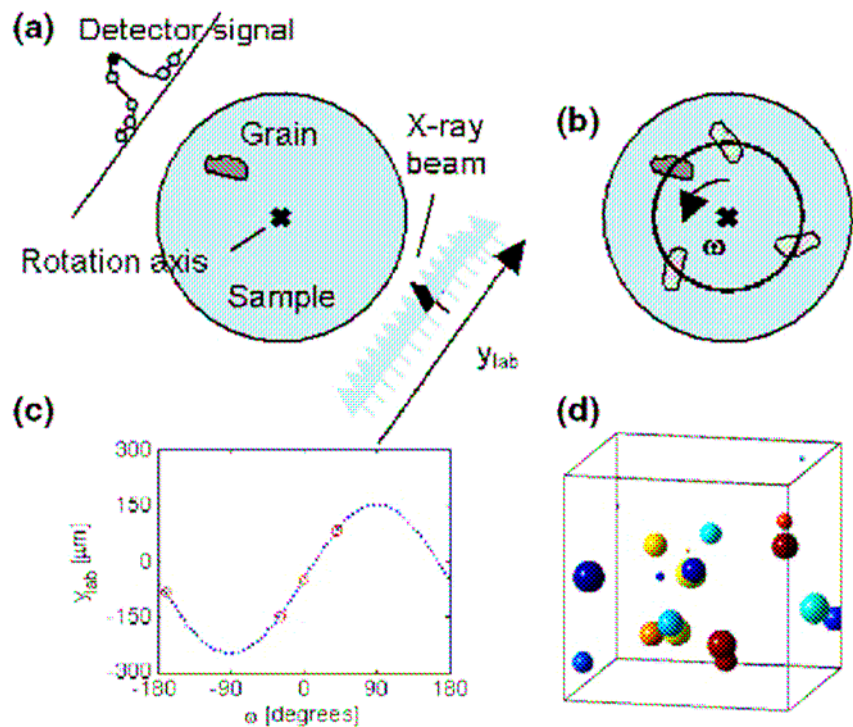


Fig. 4 Illustration of the beam scanning technique. (a) Diffraction profiles are obtained by scanning the sample through the beam both horizontally (as shown here) and vertically. (b) Repeating this procedure for a range of x-positions produces a number of reflections (projections) from each grain. (c) From the sine-curves obtained from the projections and the Grainspotter software the center-of-mass of the grain is derived. (d) Illustration of the type of output provided by the beam scanning technique: grains characterized by (x, y, z) position and spherical radius.

### **Software implementation and automation**

A main goal has been to integrate the above analysis software into a larger beamline computing structure (FABLE) to allow for automated online analysis. FABLE (Fully Automated Beamlines and Experiments) is a steering package to serve as a common platform for online data analysis and steering of the 3DXRD microscope. The online data analysis is to be carried out on a cluster of computers, where each data analysis algorithm, ranging from background subtraction to fitting geometrical parameters to mapping grain boundaries in 3D, has been embedded in a device server. FABLE distributes the workload on the cluster and writes the results in a database. In addition, FABLE utilizes a user-friendly GUI interface, allowing new users to quickly setup their experiment and analysis protocol. The workload for this task is shared between Risoe and ESRF, and has greatly benefited from regular joint meetings as part of the TotalCryst project.

FABLE is planned to be completed beginning of 2009, but a beta-version is currently used at the beamline. All programs are freely available on a sourceforge site (<http://fable.wiki.sourceforge.net/>). With respect to dissemination an "International workshop on 3DXRD: technique and applications" is planned to take place end 2008. This will include software demonstrations

### **Selected Research Highlights**

#### **Grain Growth**

During the last two years, our group has succeeded in generating the first ever 3D movies showing the coarsening behaviour of a polycrystalline sample during grain growth. We see this as a major breakthrough, allowing unprecedented options for testing numerous basic theories in the field as well as providing input data to 3D models (e.g. phase field models) of various applications. In work with C. Krill, a sample volume comprising more than 1000 grains were followed during three time steps (analysis in progress). Here we report on work with C. Maurice from St. Etienne on the annealing of an Al-0.1wt% Mn sample (paper submitted).

The material had been cold rolled 80% and pre-annealed for 8 minutes at 300 °C to produce initial grain sizes of 20 to 100 μm. The sample, cylindrical shaped with 700 μm in diameter, was then alternately annealed in an external furnace and characterized non-destructively utilizing the 3DXRD microscope. In total 5 volumes were measured with a planar shaped beam at 50 keV. Each volume contained 35 layers spaced 10 μm apart. The reconstruction of the crystallographic orientations and grain morphologies were done using the GrainSweeper algorithm. The reconstructed volume measured after the first and the final annealing are shown in Figure 5. Colours are assigned according to the crystallographic orientations of the grains.

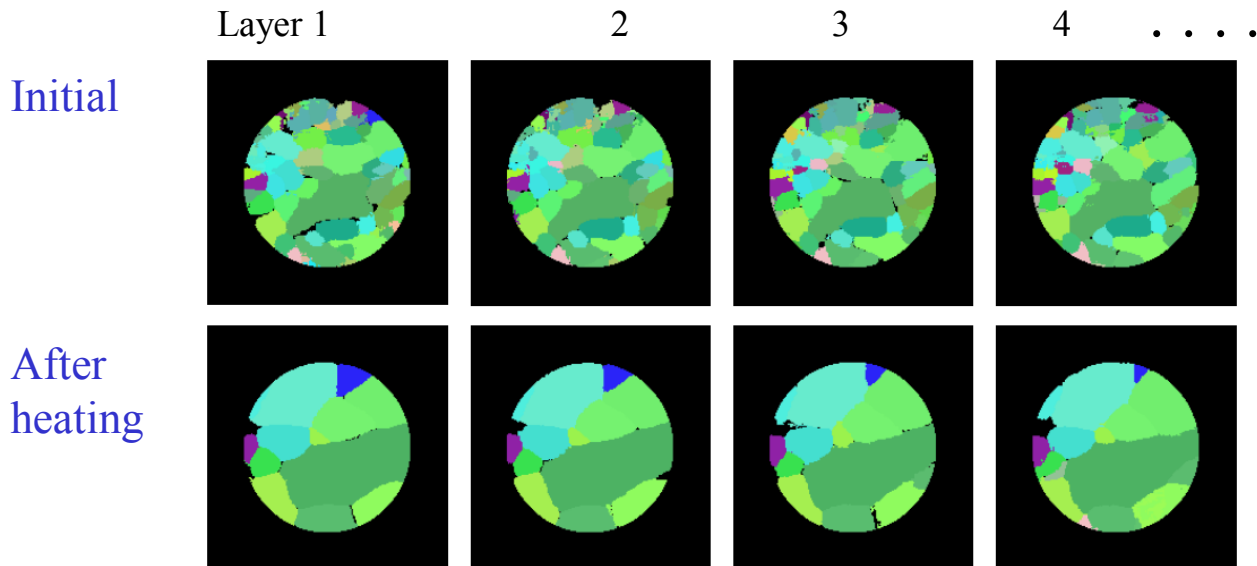


Figure 5. Layer by layer representation of the 3D grain map generated before and after annealing.

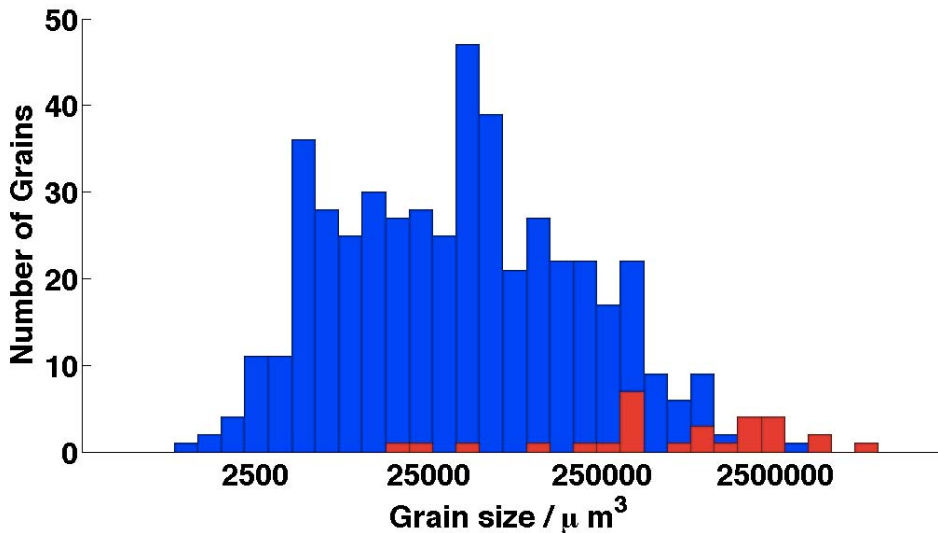


Figure 6. grain size distribution before (blue) and after (red) annealing

The 3D grain morphology as well as the crystallographic orientation was determined for 491 grains in the illuminated volume prior to annealing. The final map revealed that 30 grains had survived. The general trend is that the initial largest grains survive and the final volume size is typically 2.4 times larger than the initial volume size for the individual surviving grain. One grain, however, experiences a volume increase of a factor 14. It was shown that this grain initially is the only grain that is located in a region with many smaller surrounding grains (with evenly distributed crystallographic orientations) suggesting that the growth rate is related to the volume ratio of the growing grain to its neighbouring grains. Further analysis may answer questions such as which type of grains survive, correlations to neighbouring grains, i.e. crystallographic misorientations and grain topologies.

Another grain growth experiment in the new hutch has been performed in collaboration with C. Krill (MA-263). Due to instrumental issues and mutual scientific interests of the two groups it was decided to merge the MA-263 beamtime with 5 days of LTP beamtime on this study. With a similar set-up as above, a cylindrical Al specimen with 1.5 mm diameter was mapped within a complete 1 mm in height in three time steps, see figure 7. Reconstructions for the last step (1657 grains) has been performed. The reconstruction of the two other steps are in progress, and it found that the time steps are ideal with on average ~15% growth between annealings.

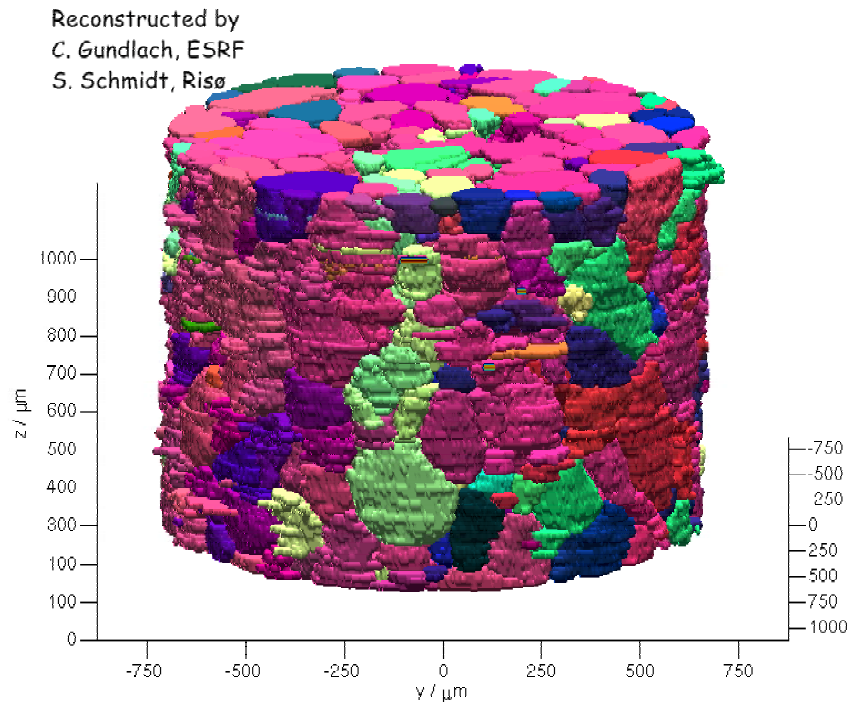


Figure 7. 3D grain reconstruction of grain growth experiment with C. Krill. The microstructure after the last annealing is shown.

### Thermal kinetics of nanomaterials

Understanding the annealing response of nanomaterials is absolutely essential for the development of structures which are thermally stable allowing the material to maintain its unique nano-properties during processing and use. For bulk nanomaterials, traditional methods such as electron microscopy can show the size scale the structure but cannot follow the dynamics. For scale coarsening, which typically occurs in pure metals, it is therefore not possible to differentiate between the basic coarsening mechanisms, recrystallization and grain growth, with these methods. By 3DXRD we have studied in-situ the coarsening kinetics of hundreds of single grains within the bulk of nanocrystalline Al (produced by cold rolling to  $e=4$ ). The results reveal that the coarsening kinetics cannot be described either by recrystallization or grain growth alone. Rather it is observed that crystallites start coarsening, and when they have reached a size of a few microns a few then break away and grow extremely quickly as seen in recrystallization, while the remainder continue to coarsen at a much lower rate. This clear dual process has not been observed before.

### Plastic deformation

Plastic deformation of polycrystalline metals induces rotation of the grains as well as increasing orientation spread within each grain. The rotation of the center of mass of individual bulk grains has previously been followed *in situ* during tensile deformation of aluminium. That study revealed that the rotation path depends strongly on the crystallographic orientation of the grain. Recently, this orientation dependence has been correlated with data on the dislocation structures evolving during deformation (Winther G., Slip systems extracted from lattice rotations and dislocation structures (in press) *Acta Materialia*) to deduce the identity of the active slip systems responsible for the rotations. Those analyses were conducted at the scale of entire grains and based on the results we now aim at investigating the developing orientation spread within each grain. More specifically the focus is on analysing for grain orientation effects and to correlate the spread with



the rotation path of the center of mass. These studies are expected to lead to significant advances in models for the behaviour of the grain seen as an isolated entity as well as its interaction with neighbouring grains.

We have developed a program to determine the orientation distribution function (ODF) for individual grains parametrized in Rodrigues space by methods similar to those in discrete tomography. After radial integration (over  $2\theta$ ) of a reflection, a so-called  $uv$  map can be made (Fig. 8). These maps are linear projections of the ODF. Hence using iterative methods (preconditioned conjugate least-squares method) the ODF can be reconstructed. We have measured data for tensile strained (2,4,6,8 and 10%) Al with a grain size of 75 microns. These conditions are similar to those used in the previous experiment on the center of mass rotation of the grains. The samples were machined cylinders ( $\phi = 400$  microns) and for each sample between 50-100 grains have been identified. As the data analysis is in progress we here show the result of the reconstruction of one of these grains from the sample strained to 6%. The ODF of this grain is shown in Fig 8. To illustrate the form of the ODF a low valued isosurface has been drawn. In Fig. 9. the distribution of the tensile axis given by the ODF of the grain has been plotted in an inverse pole figure. From comparison of this plot with the previous rotation data it is evident that the direction of primary spread of this grain is coincident with the direction of grain rotation.

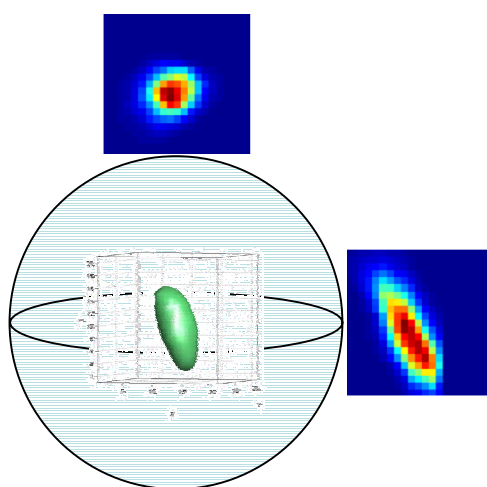


Fig. 8 Two  $uv$  maps used for the reconstruction of the ODF shown in the center of the sphere. The maps are tangential to the orientation unit sphere..

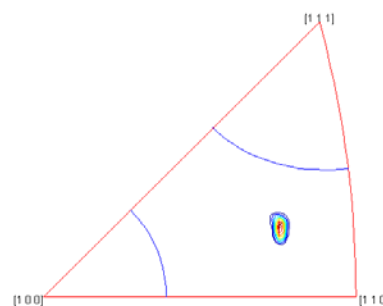


Fig. 9.. The distribution of the tensile axis given by the ODF of one bulk grain has been plotted in an inverse pole figure

### Applications in Pharmaceuticals

A main vision of the TotalCryst project – also emphasised as a key task in the LTP - is to allow routine structure solution on large molecules and particularly compounds of pharmaceutical interest from polycrystalline samples, thereby bridging the gap between routine single crystal and powder diffraction techniques.

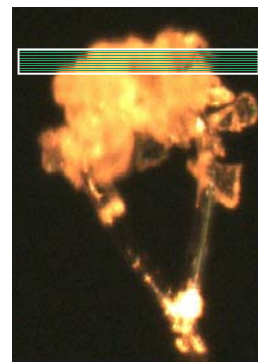


Fig. 10 BCCP crystals (size 15 microns) mounted on a cryo loop with parathene oil. The mean crystal size is about 15 microns.

In collaboration with TotalCryst partners (J. Davaasambuu, Max Planck Institute, Göttingen) progress has been made in sample handling and mounting in order to be able to collect diffraction data on weakly diffracting polycrystalline samples. Two types of mounting have been used 1) a foil of 200 nm thin Kapton and 2) a cryo loop of 50  $\mu\text{m}$  diameter, see Fig 10.

A number of test data collections have been performed with various beamline setups. Successful data collections were performed employing the new transfocator optics. The transfocator made it possible to easily optimize the beam size to the sample type. Data were collected on the polymorphs A and B of the

pharmaceutical compound 6-chloro-3-alkylamino-4H-thieno[3,2-e]-1,2,4-thiadiazine 1,1 dioxide. Although the molecular structure polymorph A has been solved by SCXRD (Nielsen, F. E. *et al.*, (2006) *J. Med. Chem.*, **49**, 4127.), polymorph B was unknown. Only the space group and unit cell parameters had been determined from powder data. A crudely refined structure of polymorph B is shown in Fig. 11. Data collections of another unknown compound, a metalorganic (it is formed by a reaction of bis(ethane-1,2-diamine)(2-iminoacetato)cobalt(III)dibromid with nitromethane in sodiumcarbonate) was performed. This compound tends to form intergrown microcrystals, hence it cannot be solved by standard crystallographic methods. To collect data on the tiny crystals (15 microns) shown in Fig. 10 of the very weakly diffracting photoactive compound BBCP, we used the Laue setup in the new hutch 3 to vertically focus the beam (height < 5 microns, beam area illustrated by the green box in Fig. 10) to maximize the beam flux on these crystals. This seems to be absolute essential on tiny organic samples in order get a signal-to-noise ratio necessary to solve the structure of these types of compounds. Data from five crystals of the bunch seen in Fig. 10 have been integrated and the structure of BBCP could be solved and refined. Details about data merging and structure refinement are shown in Table 1.

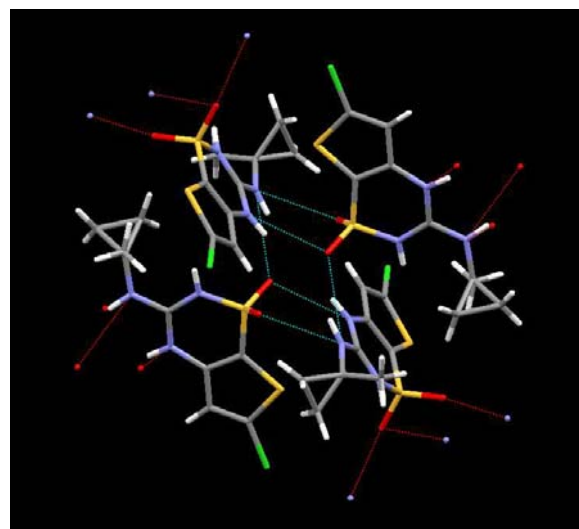


Fig. 11. Crystal packing of polymorph B of 6-chloro-3-alkylamino-4H-thieno[3,2-e]-1,2,4-thiadiazine 1,1 dioxide.

Table 1 Details of the data reduction and structure refinements of BBCP polycrystal data collection.

	Grain 1	Grain 2	Grain 3	Grain 4	Grain 5
Measured refl.	10279	20215	9538	9666	8496
Independent refl.	1373	1474	1266	1489	1165
$R_{int}, R_{\sigma}$ (%)	6.3, 2.9	39.5, 17.5	5.2, 2.6	7.8, 4.1	6.6, 3.3
Parameters refined	182	182	182	182	182
$R_1, R_w[F^2 > 2\sigma(F^2)]$ (%)	5.7, 6.3	5.8, 6.8	4.7, 5.2	6.6, 8.0	4.8, 5.7
GooF	1.072	1.028	1.057	1.039	1.039

## Peer-Reviewed International Publications from work performed at ID11

- Gundlach, C; Schmidt, S.; Margulies, L.; Knudsen, T.; Pantleon, W.; Poulsen, H.F. *Mat. Sci. Tech.* (2005) v. 21 p. 1476-1479.
- Knudsen, E., *Mat. Sci. Tech.* (2005) v. 21 p. 1376-1378
- Larsen, A.W.; Poulsen, H.F.; Margulies, L.; Gundlach, C.; Xing, Q.F.; Huang, X.; Juul Jensen, D., *Scripta Mater.* (2005) v. 53 p. 553-557
- Offerman, S.E.; Dijk, N.H. van; Sietsma, J.; Lauridsen, E.M.; Margulies, L.; Grigull, S.; Poulsen, H.F.; Zwaag, S. van der, Grenoble (FR), 23-25 Aug 2004. *Nucl. Instrum. Methods Phys. Res. B* (2005) v. 238 p. 107-110
- Schmidt, S.; Juul Jensen, D., *Arch. Metall. Mater.* (2005) v. 50 p.181-187
- Alpers, A.; Poulsen, H.F.; Knudsen, E.; Herman, G.T., *J. Appl. Cryst.* (2006) v. 39 p. 582-588
- Fu, X.; Knudsen, E.; Poulsen, H.F.; Herman, G.T.; Carvalho, B.M.; Liao, H.Y., *Opt. Eng.* (2006) v. 45, 116501 (9 p.)
- Lauridsen, E.M.; Dey, S.R.; Fonda, R.W.; Juul Jensen, D., *J. Microsc.* (2006) v. 58 p. 40-44
- Lauridsen, E.M.; Schmidt, S.; Nielsen, S.F.; Margulies, L.; Poulsen, H.F.; Juul Jensen, *Scripta Mater.* (2006) v. 55 p. 51-56

10. Offerman, S.E.; Dijk, N.H. van; Sietsma, J.; Lauridsen, E.M.; Margulies, L.; Grigull, S.; Poulsen, H.F.; Zwaag, S. van der, *Nucl. Instrum. Methods Phys. Res. B* (2006) v. 246 p. 194-200
11. Sørensen, H.O.; Jakobsen, B.; Knudsen, E.; Lauridsen, E.M.; Nielsen, S.F.; Poulsen, H.F.; Schmidt, S.; Winther, G.; Margulies, L., *Nucl. Instrum. Methods Phys. Res. B* (2006) v. 246 p. 232-237.
12. West, S.S.; Winther, G.; Margulies, L.; Knudsen, E.; Sørensen, H.O.; Schmidt, S.; Juul Jensen, D., *Mater. Sci. Forum* (2007) 558-559 , 389-394
13. Hannesson, K.; Juul Jensen, D., *Mater. Sci. Forum* (2007) 558-559 , 192-196
14. Olsen, U.L.; Badel, X.; Linnros, J.; Michiel, M. Di; Martin, T.; Schmidt, S.; Poulsen, H.F., *Nucl. Instrum. Meth. Phys. Res. A* (2007) 576 , 52-55
15. Rodek, L.; Poulsen, H.F.; Knudsen, E.; Herman, G.T., *J. Appl. Cryst.* (2007) 40 , 313-321
16. Offerman, S.E.; Strandlund, H.; Dijk, N.F. van; Sietsma, J.; Lauridsen, E.M.; Margulies, L.; Poulsen, H.F.; Ågren, J.; Zwaag, S. van der, *Mater. Sci. Forum* (2007) **550** , 357-362
17. V.I. Savran, S.E. Offerman, N.H. van Dijk, E.M. Lauridsen, L. Margulies, J. Sietsma, *Material Science Forum* 561-565 (2007) 2301-2304
18. Juul Jensen, D., *Mat. Sci. Tech.* (2005) v. 21 p. 1365-1372
19. Juul Jensen, D., *Mater. Sci. Forum* (2006) v. 519-521 p. 1569-1578

### Reviews for general Audience

1. Juul Jensen, D.; Lauridsen, E.M.; Margulies, L.; Poulsen, H.F.; Schmidt, S.; Sørensen, H.O.; Vaughan, G.B.M., X-ray microscopy in four dimensions. *Materials Today* (2006) v. 9 p. 18-25
2. Wert, J., Huang, X., Winther, W., Pantleon, W., Poulsen, H.F., *Materials Today Materials Today* (2007) v. 10 p. 24-32

### Book chapters

H.F. Poulsen, S. Schmidt and W. Ludwig in W. Reimers et al. (Eds.) *Neutrons and Synchrotron Radiation in Engineering Materials Science*. (Wiley VCH, Weinheim, 2008)

H.F. Poulsen in *Advanced Tomographic Methods in Materials Research and Engineering*, Ed.: J. Banhart (Clarendon, Oxford, 2008)

A. Alpers, L.Rodek, H.F. Poulsen, E. Knudsen, G.T. Herman. *Advances in Discrete tomography and its applications*. Eds. G.T. Herman and A. Kuba. (Birkhäuser, Boston, 2007)